

Power Management Strategy for a Parallel Hybrid Electric Truck

Chan-Chiao Lin, Huei Peng, J.W. Grizzle and Jun-Mo Kang

Chan-Chiao Lin

Ph.D. candidate

Department of Mechanical Engineering, University of Michigan

G041 Lay Automotive Laboratory, Ann Arbor, MI 48109-2121 USA

Tel: (734) 647-9732

Fax: (734) 764-4256

Email: chancl@umich.edu

Huei Peng

Professor

Department of Mechanical Engineering, University of Michigan

G036 Lay Automotive Laboratory, Ann Arbor, MI 48109-2121 USA

Tel: (734) 936-0352

Fax: (734) 764-4256

Email: hpeng@umich.edu

J. W. Grizzle

Professor

Department of Electrical Engineering and Computer Science, University of Michigan

4221 EECS Bldg., 1301 Beal Ave., Ann Arbor, MI 48109-2122, USA

Tel: (734) 763-3598

Fax: (734) 763-8041

Email: grizzle@umich.edu

Jun-Mo Kang

Ph.D.

Department of Electrical Engineering and Computer Science, University of Michigan

4430 EECS Bldg., 1301 Beal Ave., Ann Arbor, MI 48109-2122, USA

Tel: (734) 763-3092

Email: junmo@umich.edu

Index Terms — Hybrid Electric Vehicle, Power Management Strategy, Powertrain Control

Abstract

Hybrid vehicle techniques have been widely studied recently because of their potential to significantly improve the fuel economy and drivability of future ground vehicles. Due to the dual-power-source nature of these vehicles, control strategies based on engineering intuition frequently fail to fully explore the potential of these advanced vehicles. In this paper, we will present a procedure for the design of an approximately optimal power management strategy. The design procedure starts by defining a cost function, such as minimizing a combination of fuel consumption and selected emission species over a driving cycle. Dynamic Programming (DP) is then utilized to find the optimal control actions. Through analysis of the behavior of the DP control actions, approximately optimal rules are extracted, which, unlike DP control signals, are implementable. The performance of the power management control strategy is verified by using the hybrid vehicle model HE-VESIM developed at the Automotive Research Center of the University of Michigan. A trade-off study between fuel economy and emissions was performed. It was found that significant emission reduction can be achieved at the expense of a small increase in fuel consumption.

I. INTRODUCTION

Medium and heavy trucks running on diesel engines serve an important role in modern societies. More than 80% of the freight transported in the US in 1999 was carried by medium and heavy trucks. The increasing reliance on the trucking transportation brings with it certain negative impacts. First, the petroleum consumption used in the transportation sector was one of the leading contributors for the import oil gap. Furthermore, diesel-engine vehicles are known to be more polluting than gasoline-engine vehicles, in terms of NO_x (Nitrogen Oxides) and PM (Particulate Matters) emissions. Recently, hybrid electric vehicle (HEV) technology has been proposed as the basis for new vehicle configurations. Owing to their dual on-board power sources and possibility of regenerative braking, HEVs offer unprecedented potential for higher fuel economy while meeting tightened emissions standard, particularly when a parallel configuration is employed. To fully realize the potential of hybrid powertrains, the power management function of these vehicles must be carefully designed. Here, “power management” refers to the design of the higher-level, low-bandwidth control algorithm that determines the proper power level to be generated, and its split between the two power sources. In general, the control sampling time for the power management control system is low ($\sim 1\text{Hz}$). Its command then becomes the set-points for the servo-loop control systems, which operate at a much higher frequency ($>20\text{Hz}$). The servo-loop control systems can be designed for different goals, such as improved drivability, while ensuring the set-points commanded by the main loop controller are achieved reliably.

Power management strategies for parallel HEVs can be roughly classified into three categories. The first type employs intelligent control techniques such as control rules/fuzzy logic/neural networks for estimation and control algorithm development ([1], [2]). The second approach is based on static optimization methods. Commonly, electric power is translated into an equivalent amount

of (steady-state) fuel rate in order to calculate the overall fuel cost ([3], [4]). The optimization scheme then figures out the proper split between the two energy sources using steady-state efficiency maps. Because of the simple point-wise optimization nature, it is possible to extend such optimization schemes to solve the simultaneous fuel economy and emission optimization problem [5]. The basic idea of the third type of HEV control algorithms consider the dynamic nature of the system when performing the optimization ([6], [7], [8]). Furthermore, the optimization is with respect to a time horizon, rather than for an instant in time. In general, power split algorithms resulting from dynamic optimisation approaches are more accurate under transient conditions, but are computationally more intensive.

In this paper, we apply the Dynamic Programming (DP) technique to solve the optimal power management problem of a hybrid electric truck. The optimal power management solution over a driving cycle is obtained by minimizing a defined cost function. Two cases are solved: a fuel-economy only case, and a fuel/emission case. The comparison of these two cases provides insight into the change needed when the additional objective of emission reduction is included. However, the DP control actions are not implementable due to their preview nature and heavy computational requirement. They are, on the other hand, a good design tool to analyze, assess and adjust other control strategies. We study the behaviour of the dynamic programming solution carefully, and extract implementable rules. These rules are used to improve a simple, intuition-based algorithm. It was found that the performance of the rule-based algorithm can be improved significantly, and in many cases, can be made to approach the DP optimal results.

The paper is organized as follows: In Section 2, the hybrid electric truck model is described, followed by an explanation of the preliminary rule-based control strategy. The dynamic optimization problem and the DP procedure are introduced in Section 3. The optimal results for the

fuel consumption and fuel/emissions optimization cases are given in Section 4. Section 5 describes the design of improved rule-based strategies. Finally, conclusions are presented in Section 6.

II. HEV SIMULATION MODEL (HE-VESIM)

A. System Configuration

The baseline vehicle studied is the International 4700 series, a 4X2 Class VI truck. The diesel engine was downsized from a V8 (7.3L) to a V6 (5.5L) and then augmented by a 49 KW DC electric motor. An 18 amp-hour advanced valve-regulated lead-acid (VRLA) battery was chosen as the energy storage system. The hybrid truck was estimated to be 246 kg heavier than the original design. A schematic of the vehicle is given in Figure 1. The downsized engine is connected to the torque converter (TC), which in turn connects to the transmission (Trns). The transmission and the electric motor are linked to the propeller shaft (PS), differential (D) and two driveshafts (DS). Important parameters of this vehicle are given in Table 1.

Table 1: Basic vehicle parameters

DI Diesel Engine	V6, 5.475L, 157HP/2400rpm
DC Motor	49kW
Lead-acid Battery	Capacity: 18Ah
	Module number: 25
	Energy density: 34 (Wh/kg)
	Power density: 350 (W/kg)
Automatic Transmission	4 speed, GR: 3.45/2.24/1.41/1.0
Vehicle	Curb weight: 7504 kg

The Hybrid Engine-Vehicle SIMulation (HE-VESIM) model used in this paper is based on the conventional vehicle model VESIM developed at the University of Michigan [9]. VESIM was validated against measurements for a Class VI truck for both engine operation and vehicle launch/driving performance. The major changes from VESIM include the reduction of the engine size/power and corresponding fuel/emission map, and the integration of the electric components. The HE-VESIM model is implemented in SIMULINK, as presented in Figure 2. Since the model has been presented before ([9], [10]), details are omitted here.

B. Preliminary Rule Based Control Strategy

Many existing HEV power management algorithms are rule-based, because of the ease in handling switching operating modes. For parallel hybrid vehicles, there are five possible operating modes: motor only, engine only, power-assist (engine plus motor), recharging (engine charges the battery) and regenerative braking. Using the motor to start the engine occurs within short period of time and thus is not treated as a regular operating mode. In order to improve fuel economy and/or to reduce emissions, the power management controller has to decide which operating mode to use, and if proper, to determine the optimal split between the two power sources while meeting the driver's demand and maintaining battery state of charge. The simple rule-based power management strategy to be presented below was developed on the basis of engineering intuition and simple analysis of component efficiency tables/charts [8, 11], a very popular design approach. The design process starts by interpreting the driver pedal motion as a power request, P_{req} . The operation of the controller is determined by three simple rules: Braking rule, Power Split rule and Recharging rule. If P_{req} is negative, the Braking rule is applied to decelerate the vehicle. If P_{req} is positive, either the Power Split or the Recharging rule will be applied, depending on the battery state of charge (SOC). A high-level charge-sustaining strategy tries to maintain the battery SOC within defined lower and

upper bounds. A 55-60% SOC range is chosen for efficient battery operation as well as to prevent battery depletion or damage. It is important to note that these SOC levels are not hard bounds and excursions could occur. Under normal propulsive driving conditions, the Power Split rule determines the power flow in the hybrid powertrain. Whenever the SOC drops below the lower limit, the controller will switch to the Recharging rule until the SOC reaches the upper limit, and then the Power Split rule will take over. The basic logic of each control rule is described below.

Power Split Control: Based on the engine efficiency map (Figure 3), an “engine on” power line, P_{e_on} , and “motor assist” power line, P_{m_a} , are chosen to avoid engine operation in inefficient areas. If P_{req} is less than P_{e_on} , the electric motor will supply the requested power alone. Beyond P_{e_on} , the engine becomes the sole power source. Once P_{req} exceeds P_{m_a} , engine power is set at P_{m_a} and the motor is activated to make up the difference ($P_{req} - P_{m_a}$).

Recharging Control: In addition to powering the vehicle, the engine sometimes needs to provide additional power to charge the battery. Commonly, a pre-selected recharge power level, P_{ch} , is added to the driver’s power request which becomes the total requested engine power. The motor power command becomes negative ($P_m = -P_{ch}$). However, this simple rule is frequently found to be inefficient, and exceptions must be allowed. One example is that when P_{req} is less than P_{e_on} , the recharging mode might not be activated. If the SOC is not excessively low, the motor will still propel the vehicle to prevent inefficient engine operation. The other exception is that when P_{req} is greater than P_{m_a} , the motor power will become positive to assist the engine, or stay at zero (when SOC is too low).

Braking Control: When P_{req} is negative, regenerative braking is activated. If P_{req} exceeds the regenerative braking capacity P_{m_min} , friction brakes will assist the deceleration ($P_b = P_{req} - P_{m_min}$).

C. Fuel Economy and Emissions Evaluation

Unlike light-duty hybrid vehicles, heavy-duty hybrid vehicles do not yet have a standardized test procedure for measuring their emissions and fuel economy performance. A test protocol is under development by SAE and NAVC based on SAE J1711 [16] at the time of the writing of this paper. Therefore, it was decided to adopt the procedures proposed in [17]. The chassis-based driving schedule for heavy-duty vehicles (UDDSHDV), as opposed to an engine-only dynamometer cycle, is adopted. For UDDSHDV, emissions are recorded and reported in the unit of gram per mile (g/mi). In addition, the battery SOC correction procedure proposed in [17] is used to correct fuel economy and emissions. The hybrid electric truck with the preliminary rule-based controller was tested through simulation over the UDDSHDV cycle. Table 2 compares the results of the HEV with those of the conventional diesel engine truck. It can be seen that the hybrid-electric truck, under the preliminary rule based control algorithm, achieves 27% better fuel economy compared to the baseline diesel truck. A 10% PM reduction is also achieved even though no emission criterion is explicitly included; this is primarily due to the effect of improved fuel economy. NOx level increases because the engine works harder. In fact, this is exactly the main point of this paper: it is hard to include more than one objective in simple rule-based control strategies, which are commonly driven by intuition and trial-and-error. Such a simple control strategy is not optimal since it is usually component-based as oppose to system-based. Usually we do not even know how much room is left for improvement. This motivates the use of Dynamic Programming as an analysis and design tool.

Table 2: Performance comparison: conventional vs. HEV

	FE (mi/gal)	NOx (g/mi)	PM (g/mi)
Conventional Truck	10.34	5.347	0.508
Hybrid Truck (Preliminary Rule-Base)	13.11	5.770	0.460

III. DYNAMIC OPTIMIZATION PROBLEM

Contrary to rule-based algorithms, the dynamic optimization approach relies on a dynamic model to compute the best control strategy. For a given driving cycle, the optimal operating strategy to minimize fuel consumption, or combined fuel consumption/emissions can be obtained. A numerical-based Dynamic Programming (DP) approach is adopted in this paper to solve this finite horizon optimization problem.

A. Problem Formulation

In the discrete-time format, a model of the hybrid electric vehicle can be expressed as:

$$x(k+1) = f(x(k), u(k)) \quad (1)$$

where $u(k)$ is the vector of control variables such as fuel injection rate to the engine, desired output torque from the motor, and gear shift command to the transmission. $x(k)$ is the state vector of the system. The sampling time for this main-loop control problem is selected to be one second. The optimization goal is to find the control input, $u(k)$, which minimizes a cost function, which consists of the weighted sum of fuel consumption and emissions for a given driving cycle. The cost function to be minimized has the following form:

$$J = \sum_{k=0}^{N-1} L(x(k), u(k)) = \sum_{k=0}^{N-1} \text{fuel}(k) + \mu \cdot \text{NOx}(k) + \nu \cdot \text{PM}(k) \quad (2)$$

where N is the duration of the driving cycle, and L is the instantaneous cost including fuel use and engine-out NOx and PM emissions. For a fuel-only problem, $\mu = \nu = 0$, and $\mu > 0$, $\nu > 0$ for a simultaneous fuel/emission problem.

During the optimization, it is necessary to impose certain inequality constraints to ensure safe/smooth operation of the engine/battery/motor. The four (or more precisely, eight) constraints we imposed are:

$$\begin{aligned} \omega_{e_min} &\leq \omega_e(k) \leq \omega_{e_max} \\ T_{e_min}(\omega_e(k)) &\leq T_e(k) \leq T_{e_max}(\omega_e(k)) \\ T_{m_min}(\omega_m(k), SOC(k)) &\leq T_m(k) \leq T_{m_max}(\omega_m(k), SOC(k)) \\ SOC_{min} &\leq SOC(k) \leq SOC_{max} \end{aligned} \quad (3)$$

where ω_e is the engine speed, T_e is the engine torque, T_m is the motor torque and SOC is the battery state of charge. In addition, we also impose two equality constraints for the optimization problem, so that the vehicle always meets the speed and load (torque) demands of the driving cycle at each sampling time.

The above problem formulation does not impose any constraint on terminal SOC, the optimization algorithm tends to deplete the battery in order to attain minimal fuel consumption. Hence, a terminal constraint on SOC needs to be imposed as well:

$$\begin{aligned} J &= \sum_{k=0}^{N-1} [L(x(k), u(k))] + G(x(N)) \\ &= \sum_{k=0}^{N-1} [\text{fuel}(k) + \mu \cdot \text{NOx}(k) + \nu \cdot \text{PM}(k)] + \alpha (SOC(N) - SOC_f)^2 \end{aligned} \quad (4)$$

where SOC_f is the desired SOC at the final time (which is usually equal to the initial SOC), and α is a positive weighting factor.

B. Model Simplification

The detailed HE-VESIM model (24 states) is not suitable for dynamic optimization due to its high number of states (curse of dimensionality). Thus, a simplified (complex enough) vehicle model is developed. Due to the selection of the sampling time ($T=1\text{sec}$), dynamics that are much faster than 1Hz could be ignored. By analyzing the dynamic modes, it was determined that only two state variables needed to be kept: the transmission gear number and the battery SOC. The simplifications of the five sub-systems: engine, driveline, transmission, motor/battery and vehicle are described below.

1) Engine: The engine dynamics are ignored and the output torque generated is from a look-up table with two independent variables: engine speed and fuel injected per cylinder/cycle [9]. The feed-gas NOx and PM emissions are functions of engine torque and engine speed and are obtained by scaling the emission maps from the Advisor program [18].

2) Driveline: The driveline components are fast and thus were reduced to static models.

$$T_p = \left(\frac{\omega_e}{K(\omega_r)} \right)^2, \quad T_t = T_r(\omega_r) \cdot T_p \quad (5)$$

$$T_x = (T_t - T_{x,l1} - T_{x,l2}(\omega_t, g_x)) \cdot R_x(g_x) \cdot \eta_x(g_x) \quad (6)$$

$$T_d = (T_x + R_c \cdot T_m \cdot \eta_c - T_{d,l}(\omega_x)) \cdot R_d \cdot \eta_d \quad (7)$$

where T_p and T_t are pump and turbine torques, K and T_r are the capacity factor and torque ratio of the torque converter, $\omega_r = \omega_t / \omega_e$ is the speed ratio of the torque converter, T_x and T_d are the

output torque of the transmission and differential, respectively. R_x and η_x are gear ratio and efficiency of the transmission, which are functions of the gear number, g_x .

3) *Transmission*: The automatic transmission is modeled as a ratio device with gear number as the sole state. The control ('*shift*') to the transmission is constrained to take on the values of -1 , 0 , and 1 , representing downshift, sustain and up-shift, respectively. The gear shift dynamics are then described by:

$$g_x(k+1) = g_x(k) + shift(k) \quad (8)$$

4) *Motor/Battery*: The electric motor characteristics are based on the efficiency data obtained from the Advisor program [18] as shown in Figure 4. The efficiency of the motor is a function of motor torque and motor speed, $\eta_m = f(T_m, \omega_m)$. However, due to the battery power and motor torque limit, the final motor torque becomes:

$$T_m = \begin{cases} \min(T_{m,req}, T_{m,dis}(\omega_m), T_{bat,dis}(SOC, \omega_m)) & T_{m,req} > 0 \\ \max(T_{m,req}, T_{m,chg}(\omega_m), T_{bat,chg}(SOC, \omega_m)) & T_{m,req} < 0 \end{cases} \quad (9)$$

where $T_{m,req}$ is the requested motor torque, $T_{m,dis}$ and $T_{m,chg}$ are the maximum motor torque in the motoring and charging modes, and $T_{bat,dis}$ and $T_{bat,chg}$ are the torque bounds due to battery current limit in the discharging and charging modes.

Of all the sub-systems, the battery is perhaps the least understood. The reason is that the battery performance—voltage, current and efficiency as manifested from a purely electric viewpoint - is the outcome of thermally-dependent electrochemical processes that are quite complicated. Various models have been developed in the literature. If we ignore thermal-temperature effects and

transients (due to internal capacitance), the battery model reduces to a static equivalent circuit shown in Figure 5. The only state variable left in the battery is the state of charge (SOC):

$$SOC(k+1) = SOC(k) - \frac{V_{oc} - \sqrt{V_{oc}^2 - 4(R_{int} + R_t) \cdot T_m \cdot \omega_m \cdot \eta_m}}{2(R_{int} + R_t) \cdot Q_b} \quad (10)$$

where the internal resistance, R_{int} , and the open circuit voltage, V_{oc} , are functions of the battery SOC, Q_b is the maximum battery charge and R_t is the terminal resistance. The battery plays an important role in the overall performance of HEVs because of its nonlinear, non-symmetric and relatively low efficiency characteristics. Figure 6 shows the charging and discharging efficiency of the battery. It can be seen that discharging efficiency decreases at low SOC and charging efficiency decreases at high SOC region. Overall, the battery operates more efficiently at low power levels in both charging and discharging.

5) *Vehicle*: The vehicle is modelled as a point-mass:

$$v_v(k+1) = v_v(k) + \frac{1}{M_r} \left(\frac{T_{wh}(k)}{r_d} - \frac{B_{wh}v_v(k)}{r_d^2} - \frac{v_v(k)}{|v_v(k)|} (F_r + F_a(v_v(k))) \right) \quad (11)$$

where v_v is the vehicle speed, T_{wh} is the net wheel torque from the driveline and the hydraulic brake, r_d is the dynamic tire radius, B_{wh} is the viscous damping, F_r and F_a are the rolling resistance force and the aerodynamic drag force, $M_r = M_v + J_r / r_d^2$ is the effective mass of the vehicle, and J_r is the equivalent moment of inertia of the rotating components in the vehicle.

C. Dynamic Programming Method

Based on Bellman's principle of optimality, the DP solution for the cost function shown in Eq.(4) is [12]:

Step $N-1$:

$$J_{N-1}^*(x(N-1)) = \min_{u(N-1)} [L(x(N-1), u(N-1)) + G(x(N))] \quad (12)$$

Step k , for $0 \leq k < N-1$

$$J_k^*(x(k)) = \min_{u(k)} [L(x(k), u(k)) + J_{k+1}^*(x(k+1))] \quad (13)$$

The recursive equation is solved backwards to find the optimal control policy. Each of the indicated minimizations is performed subject to the inequality constraints shown in Eq. (3) and the equality constraints imposed by the driving cycle. A standard way to solve the above DP problem numerically is to use quantization and interpolation ([12], [13]). The state and control values are first quantized into finite grids. At each step of the optimization search, the function $J_k(x(k))$ is evaluated only at the grid points of the state variables. If the next state, $x(k+1)$, does not fall exactly on to a quantized value, then the values of $J_{k+1}^*(x(k+1))$ in Eq.(13) as well as $G(x(N))$ in (12) are determined through interpolation.

Despite the use of a simplified model, and a quantized search space, the long time horizon makes the above algorithm computationally expensive. In this research, we adopted two “tricks” to accelerate the optimization search. First, from the velocity profile of the driving cycle, the required wheel torque $T_{wh,req}$ is determined by inversely solving Eq.(11). The wheel speed $\omega_{wh,req}$ can be computed by feeding the required wheel torque to the vehicle model in order to include the wheel dynamics and slip effect. Combining this procedure with the defined state/input grid, the vehicle model can be replaced by a finite set of operating points parameterized by $T_{wh,req}$ and $\omega_{wh,req}$. The second trick adopted is to construct pre-computed look-up tables for the new states and instantaneous cost as a function of quantized states, control inputs, and operating points. Once these

tables are built, they can be used to update Eq.(13) efficiently by the vector operations in MATLAB [13].

IV. DYNAMIC PROGRAMMING RESULTS

The DP procedure described above produces an optimal, time-varying, state-feedback control policy, i.e., $u^*(x(k), k)$. It should be noted that DP creates a family of optimal paths for all possible initial conditions. Once the initial SOC is specified, the optimal policy will find a way to achieve the minimal weighted cost of fuel consumption and emissions while bringing the final SOC close to the desired terminal value (SOC_f). The optimal control policy was applied to the full-order HEVESIM model for final evaluation. In the following, two cases are presented: fuel economy only, and simultaneous fuel/emission optimization.

A. Fuel Economy Optimization Results

The weightings in Eq.(4) are chosen to be $\mu = 0, \nu = 0, \alpha = 5 \cdot 10^6$ for this case. The UDDSHDV driving cycle is again used. The initial and terminal SOC were both selected to be 0.57. Simulation results of the vehicle under the DP policy are shown in Figure 7. There is a small difference (<2mph) between the desired vehicle speed (UDDSHDV) and the achieved vehicle speed, caused by model mismatch and the long sampling time (1 sec). The engine power and motor power trajectories represent the optimal operation between two power movers for achieving the best fuel economy. An additional 6% fuel economy improvement was achieved by the DP algorithm (Table 3) as compared with the values shown in Table 2.

Table 3: Summary of DP results

	FE (mi/gal)	Fuel (g/mi)	NOx (g/mi)	PM (g/mi)
$\mu = 0, \nu = 0$	13.71	234.71	5.627	0.446

B. Fuel Economy and Emissions Optimization

To study the trade-off between fuel economy and emissions, the weighting factors are varied:

$$\begin{aligned} \mu &\in \{0, 5, 10, 20, 40\} \\ \nu &\in \{0, 100, 200, 400, 600, 800\} \end{aligned} \tag{14}$$

Selected optimization results are shown in Figures 8 and 9. The case of $\mu = \nu = 0$ corresponds to the optimal fuel economy scenario. Figure 8 shows the trade-off in NOx emissions and fuel economy. Increasing μ leads to significant NOx reduction while causing a small fuel economy increase. Increasing ν results in reduced PM (Figure 9) but higher NOx emissions and lower fuel economy (Figure 8). The trade-off between NOx and PM can be seen from Figure 9 where larger ν tends to decrease PM emission but increase NOx emission. More importantly, significant reduction in NOx and PM emissions can be achieved at the price of a small increase in fuel consumption.

The values of $\mu = 40, \nu = 800$ seem to achieve a good trade-off--NOx and PM are reduced by 17.3 % and 10.3% respectively at a 3.67% penalty on fuel economy. Simulation results of this case are shown in Figure 10. The SOC fluctuates in a wider range compared to the fuel-only case (Figure 7). It can be seen that in the case of fuel-only optimization, almost all of the negative motor power is due to regenerative braking. In other words, the engine seldom recharges the battery. Therefore, all electrical energy consumed comes from regenerative braking. This implies that it is not efficient to use engine power to charge the battery. This is due to the fact that the fuel efficiency map of this diesel engine is flat in medium to high power regions.

V. DEVELOPMENT OF IMPROVED RULE-BASED CONTROLS

The DP control policy is not implementable in real driving conditions because it requires knowledge of future speed and load profile. Nonetheless, analyzing its behaviour provides useful insight into possible improvement of the rule-based controller.

A. Gear Shift Control

The gear-shifting schedule is crucial to the fuel economy of hybrid electric vehicles [14]. In the Dynamic Programming scheme, gear-shift command is one of the control variables. It is interesting to find out how the DP solution chooses the optimal gear position to improve fuel economy and reduce emissions. It is first observed that the optimal gear trajectory has frequent shifting, which is undesirable. Hence, a drivability constraint is added to avoid this:

$$J = \sum_{k=0}^{N-1} \left(fuel(k) + 40 \cdot NOx(k) + 800 \cdot PM(k) + \beta \cdot |g_x(k+1) - g_x(k)| \right) + 5 \cdot 10^6 \cdot (SOC(N) - SOC_f)^2 \quad (15)$$

where β is a positive weighting factor. Figure 11 shows the optimal gear position trajectories from DP for different values of β . It can be seen that a larger value of β results in less frequent gear shifting. The value of $\beta = 1.5$ is chosen.

From the DP results, the gear operational points are plotted on the engine power demand vs. transmission speed plot (Figure 12). It can be seen that the gear positions are separated into four regions and the boundary between adjacent regions represent optimal gear shifting thresholds. After adding a hysteresis function to the shifting thresholds, a new gear shift map is obtained. It should be mentioned that the optimal gear shift map can also be constructed through static

optimization ([11], [15]). Given an engine power and wheel speed, the best gear position for minimum weighted cost of fuel and emissions can be chosen based on the combined steady-state engine fuel consumption and emissions map. It is found that the steady-state gear map from this method nearly coincides with Figure 12.

B. Power Split Control

In this section, we study how Power Split Control of the preliminary rule-based strategy can be improved. A power-split-ratio $PSR = \frac{P_{eng}}{P_{req}}$ is defined to quantify the positive power flows in the powertrain, where P_{eng} is the engine power and P_{req} is the power request from the driver. Four positive-power operating modes are defined: motor-only ($PSR = 0$), engine-only ($PSR = 1$), power-assist ($0 < PSR < 1$), and recharging mode ($PSR > 1$). The optimal (DP) behavior uses the motor-only mode in the low power-demand region at vehicle launch. When the wheel speed is above 6 rad/s, a simple rule is found by plotting the optimal PSR versus the power request over the transmission input speed, which is equivalent to torque demand at the torque converter output shaft (see Figure 13). The figure shows the optimal policy uses the recharging mode ($PSR > 1$) in the low torque region, the engine-only mode in the middle torque region, and the power-assist mode in the high torque region. This can be explained by examining a weighted Brake Specific Fuel and Emissions Consumption (BSFEC) of the engine.

$$BSFEC = \frac{W_f + \mu \cdot W_{NOx} + \nu \cdot W_{PM}}{P_{eng}} \quad (16)$$

The contour of engine BSFEC map is shown in the Figure 14. It can be seen that the best BSFEC region occurs at low torque levels. In order to move the engine operating points towards a better BSFEC region, the engine is used to recharge the battery at low load, and the motor is used to assist

the engine at high load. In order to extract an implementable rule, a least-square curve fit is used to approximate the optimal PSR, shown as the solid line in Figure 13.

C. Charge-Sustaining Strategy

The Power Split Control scheme described above does not maintain the battery SOC within desired operating range. An additional rule should be developed to prevent the battery from over depleting or overcharging. The strategy for regulating the SOC still needs to be obtained in an approximately optimal manner in order to satisfy the overall goal: minimize fuel consumption and emissions. The DP procedure is repeated again except this time the regenerative braking function is turned off. In other words, no “free” energy from the regenerative braking is available to recharge the battery. After the optimisation, the curve-fit optimal PSR result is computed as before, and compared with the result that included regenerative braking. Figure 15 shows the recharging part is still important even with no regenerative braking energy supplied. This is because increasing the engine power can move the engine’s operation to the best BSFEC region; the excess energy is stored for later use by the motor during the high power demand. On the other hand, with the regenerative energy, the electric motor can act more aggressively to share the load with the engine since running the engine in high power is unfavourable to the fuel economy and emissions reduction. As a result, knowing the amount of the regenerative braking energy the vehicle will capture in future driving is the key to achieve the best fuel and emissions reduction while maintaining the battery SOC level. However, estimating the future amount of regenerative energy is not easy since future driving conditions are usually unknown. An alternative is to adjust the control strategy as a function of the battery SOC. More aggressive spending of battery energy can be used when SOC is high and more conservative rules can be used when SOC is low. These

adaptive PSR rules can be learned from DP results by specifying different initial SOC points to simulate the optimal operation to bring the SOC back to its nominal value.

D. Performance Evaluation

After incorporating all the changes outlined in the previous sections, the improved rule-based controller is evaluated using several different driving cycles. In addition to the original cycle (UDDSHDV), the new rule-based controller, without change, is evaluated on three other driving cycles (suburban, interstate, and city) to test its robustness. The results are shown in Tables 4-7. It can be seen that depending on the nature of the driving cycles, the new rule-based control system may not improve all three categories of performance, and in certain cases did worse. However, if the combined fuel/emission performance is considered (the “performance measure”), the new rule-based controller is always significantly better than the original, intuition driven rule-based control law.

Table 4: Results over the UDDSHDV cycle

	FE (mi/gal)	NOx (g/mi)	PM (g/mi)	Performance Measure *
Baseline Rule-Based	13.16	5.740	0.458	840.63
New Rule-Based	12.82	4.866	0.435	793.16
DP (FE & Emis)	13.24	4.642	0.399	739.56

Performance Measure: $fuel + 40 \cdot NOx + 800 \cdot PM$ (g/mi)

Table 5: Results over the WVUSUB cycle

	FE (mi/gal)	NOx (g/mi)	PM (g/mi)	Performance Measure
Baseline Rule-Based	15.31	4.429	0.355	671.23
New Rule-Based	14.61	3.021	0.300	582.18
DP (FE & Emis)	15.41	2.779	0.259	526.67

Table 6: Results over the WVUINTER cycle

	FE (mi/gal)	NOx (g/mi)	PM (g/mi)	Performance Measure
Baseline Rule-Based	12.84	7.285	0.509	948.83
New Rule-Based	12.72	6.309	0.488	896.00
DP (FE & Emis)	12.97	6.168	0.441	847.67

Table 7: Results over the WVUCITY cycle

	FE (mi/gal)	Nox (g/mi)	PM (g/mi)	Performance Measure
Baseline Rule-Based	16.18	3.870	0.332	621.22
New Rule-Based	15.09	2.487	0.228	494.12
DP (FE & Emis)	16.63	2.037	0.161	403.58

VI. CONCLUSIONS

Designing the power management strategy for HEV by approximately extracting rules from the Dynamic Programming (DP) results has the clear advantage of being near-optimal, accommodating multiple objectives, and systematic. Depending on the overall objective, one can easily develop power management laws that emphasize fuel economy, and/or emissions. By analyzing the DP results, an improved rule-based control strategy can be developed. The extracted rules were found to be robust, rather than cycle-specific. This is evident by the fact that the rules based on one cycle work extremely well for several never-seen driving cycles, moving the rule-based control law closer to the theoretically optimal (DP) results by 50-70%.

ACKNOWLEDGMENT

This research is supported by the U.S. Army TARDEC under the contract DAAE07-98-C-R-L008. The work of J.W. Grizzle was supported in part by NSF contract IIS-9988695.

REFERENCES

- [1] B. M. Baumann, G. N. Washington, B. C. Glenn, and G. Rizzoni, "Mechatronic Design and Control of Hybrid Electric Vehicles," *IEEE/ASME Transactions on Mechatronics*, vol. 5 no. 1, pp. 58-72, 2000
- [2] S. D. Farrall and R. P. Jones, "Energy Management in an Automotive Electric/Heat Engine Hybrid Powertrain Using Fuzzy Decision Making," *Proceedings of the 1993 International Symposium on Intelligent Control*, Chicago, IL, 1993.
- [3] C. Kim, E. NamGoong, and S. Lee, "Fuel Economy Optimization for Parallel Hybrid Vehicles with CVT," *SAE Paper* No. 1999-01-1148.
- [4] G. Paganelli, G. Ercole, A. Brahma, Y. Guezennec, and G. Rizzoni, "A General Formulation for the Instantaneous Control of the Power Split in Charge-Sustaining Hybrid Electric Vehicles." *Proceedings of 5th Int'l Symposium on Advanced Vehicle Control*, Ann Arbor, MI, 2000.
- [5] V.H. Johnson, K. B. Wipke, and D.J. Rausen, "HEV Control Strategy for Real-Time Optimization of Fuel Economy and Emissions," *SAE Paper* No. 2000-01-1543, April 2000.
- [6] A. Brahma, Y. Guezennec, and G. Rizzoni, "Dynamic Optimization of Mechanical Electrical Power Flow in Parallel Hybrid Electric Vehicles," *Proceedings of 5th Int'l Symposium on Advanced Vehicle Control*, Ann Arbor, MI, 2000.
- [7] U. Zoelch and D. Schroeder, "Dynamic Optimization Method for Design and Rating of the Components of a Hybrid Vehicle," *International Journal of Vehicle Design*, vol. 19, no. 1, pp. 1-13, 1998.
- [8] C. Lin, J. Kang, J. W. Grizzle, and H. Peng, "Energy Management Strategy for a Parallel Hybrid Electric Truck," *Proceedings of the 2001 American Control Conference*, Arlington, VA, June, 2001, pp. 2878-2883.
- [9] D.N. Assanis, Z. S. Filipi, S. Gravante, D. Grohnke, X. Gui, L. S. Louca, G. D. Rideout, J. L. Stein, and Y. Wang, "Validation and Use of SIMULINK Integrated, High Fidelity, Engine-In-Vehicle Simulation of the International Class VI Truck," *SAE Paper* No. 2000-01-0288, 2000.

- [10]C. Lin, Z. S. Filipi, Y. Wang, L. S. Louca, H. Peng, D. N. Assanis, and J. L. Stein, “Integrated, Feed-Forward Hybrid Electric Vehicle Simulation in SIMULINK and its Use for Power Management Studies”, *SAE Paper* No. 2001-01-1334, 2001.
- [11]P. D. Bowles, “Modeling and Energy Management for a Parallel Hybrid Electric Vehicle (PHEV) with Continuously Variable Transmission (CVT),” MS thesis, University of Michigan, Ann Arbor, MI, 1999
- [12]D. P. Bertsekas, *Dynamic Programming and Optimal Control*, Athena Scientific, 1995
- [13]J. Kang, I. Kolmanovsky and J. W. Grizzle, “Dynamic Optimization of Lean Burn Engine Aftertreatment,” *ASME J. Dynamic Systems Measurement and Controls*, Vol. 123, No. 2, pp. 153-160, Jun. 2001.
- [14]H. D. Lee, S. K. Sul, H. S. Cho, and J. M. Lee, “Advanced Gear Shifting and Clutching Strategy for Parallel Hybrid Vehicle with Automated Manual Transmission,” *Proceedings of the IEEE Industry Applications*, 1998.
- [15]P. Soltic and L. Guzzella, "Optimum SI Engine Based Powertrain Systems for Lightweight Passenger Cars," *SAE Paper* No. 2000-01-0827, 2000
- [16]Society of Automotive Engineers, Hybrid-Electric Vehicle test Procedure Task Force, “SAE J1711, Recommended Practice for Measuring Exhaust Emissions and Fuel Economy of Hybrid-Electric Vehicles,” 1998.
- [17]D. L. Mckain, N. N. Clark, T. H. Balon, P. J. Moynihan, P. J. Lynch, and T. C. Webb, "Characterization of Emissions from Hybrid-Electric and Conventional Transit Buses," *SAE Paper* 2000-01-2011, 2000
- [18]National Renewable Energy Laboratory, “ADVISOR 3.2 Documentation,” <http://www.ctts.nrel.gov/analysis/>, 2001.

Chan-Chiao Lin, Huei Peng, J.W. Grizzle and Jun-Mo Kang: Figure Captions

List of Figure Captions

Figure 1: Schematic diagram of the hybrid electric truck.

Figure 2: Vehicle model in SIMULINK.

Figure 3: Power Split Control rule.

Figure 4: Efficiency map of the electric motor.

Figure 5: Static equivalent circuit battery model.

Figure 6: Efficiency maps of the lead acid battery: discharging (left) and charging (right).

Figure 7: Simulation results for the fuel-economy-only case.

Figure 8: Fuel economy versus engine-out NO_x emissions.

Figure 9: Engine-out PM emissions versus NO_x emissions

Figure 10: Simulation results ($\mu = 40, \nu = 800$).

Figure 11: Optimal gear position trajectory.

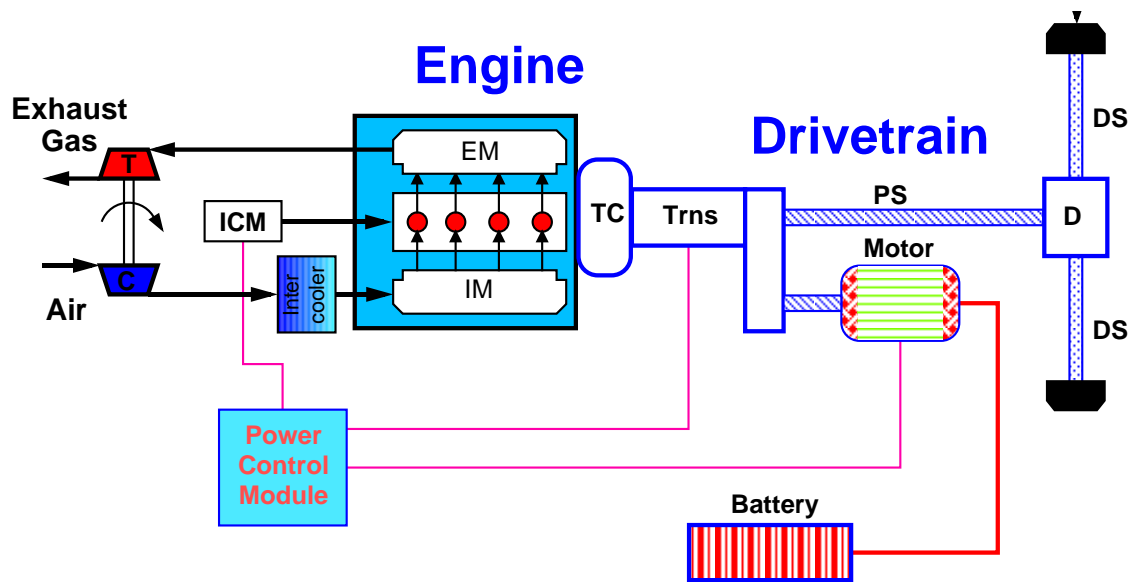
Figure 12: Gear operating points of DP optimisation.

Figure 13: DP power split behavior (UDDSHDV cycle).

Figure 14: BSFEC map in g/kWhr.

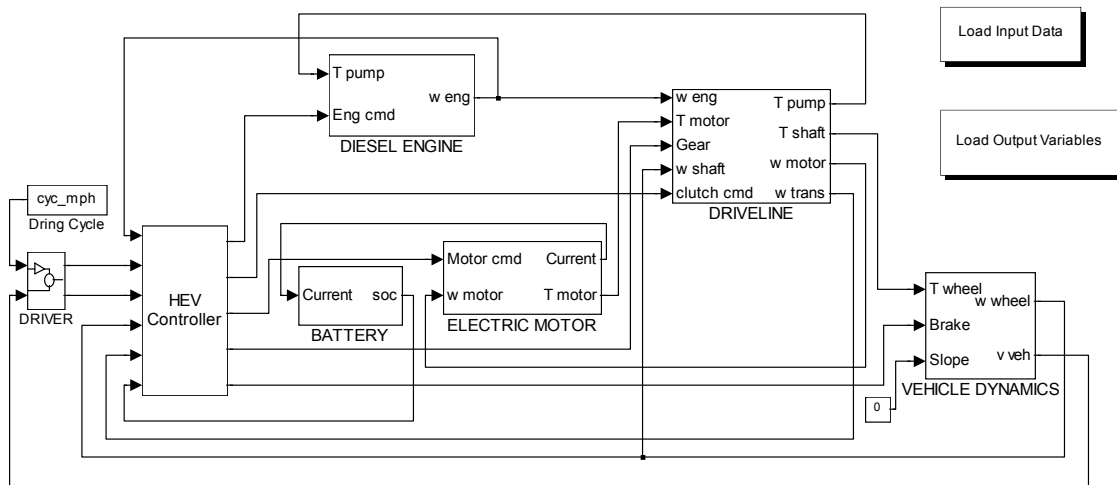
Figure 15: Optimal PSR rules comparison.

Chan-Chiao Lin, Hwei Peng, J.W. Grizzle and Jun-Mo Kang: Figure 1

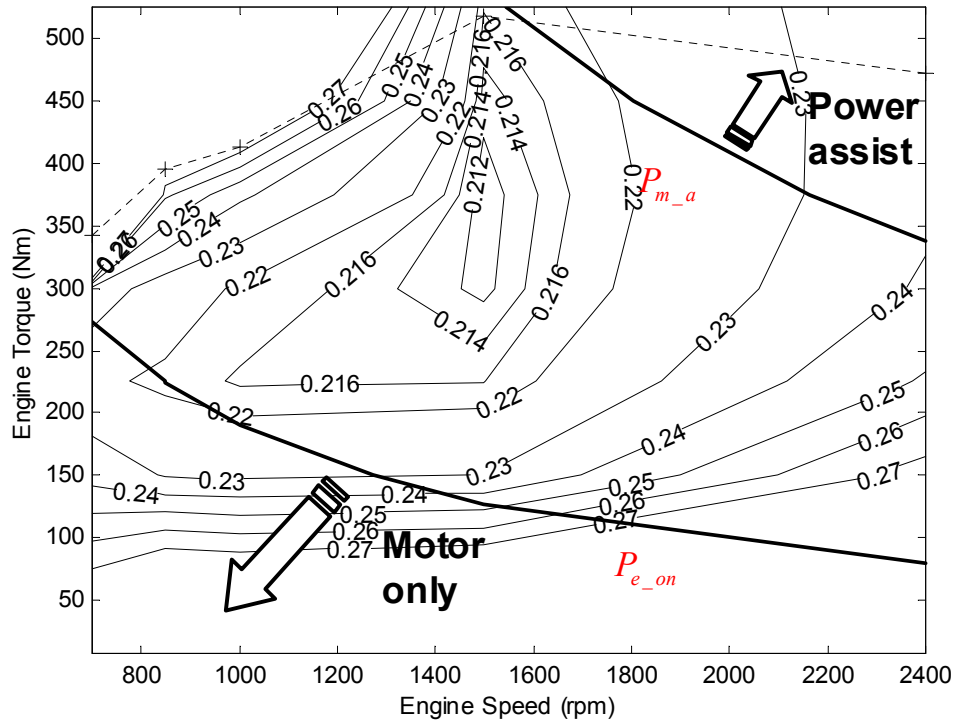


Power Management Strategy for a Parallel Hybrid Electric Truck

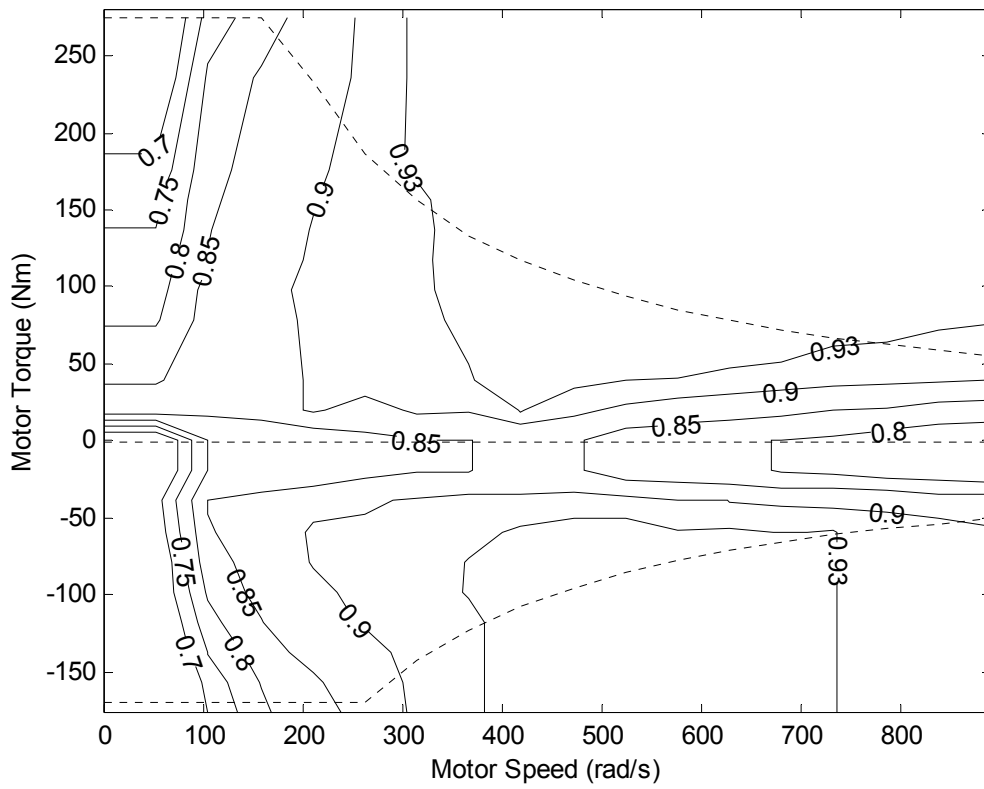
Chan-Chiao Lin, Huei Peng, J.W. Grizzle and Jun-Mo Kang: Figure 2



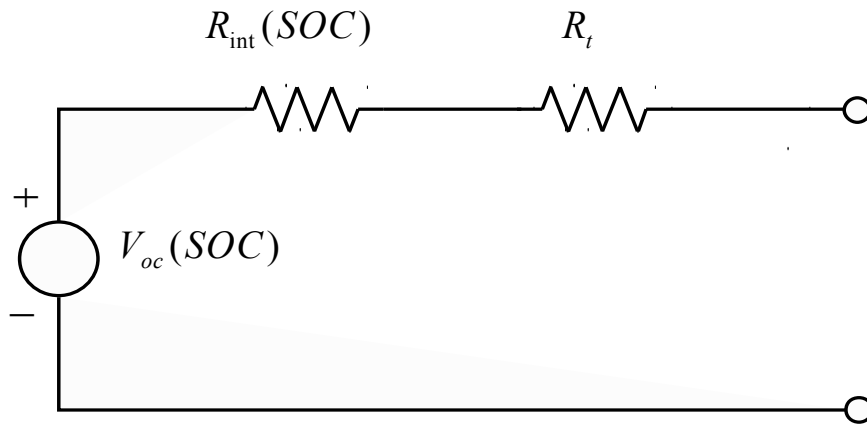
Chan-Chiao Lin, Hwei Peng, J.W. Grizzle and Jun-Mo Kang: Figure 3



Chan-Chiao Lin, Hwei Peng, J.W. Grizzle and Jun-Mo Kang: Figure 4

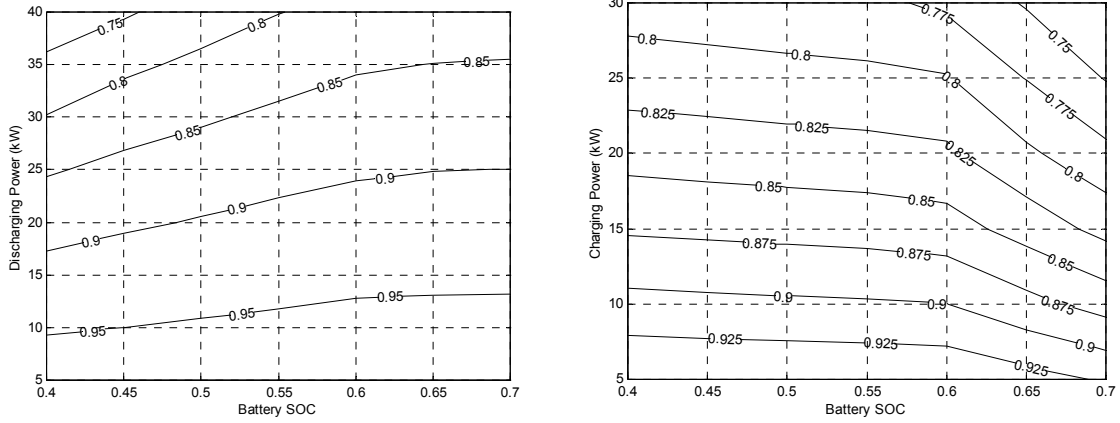


Chan-Chiao Lin, Huei Peng, J.W. Grizzle and Jun-Mo Kang: Figure 5

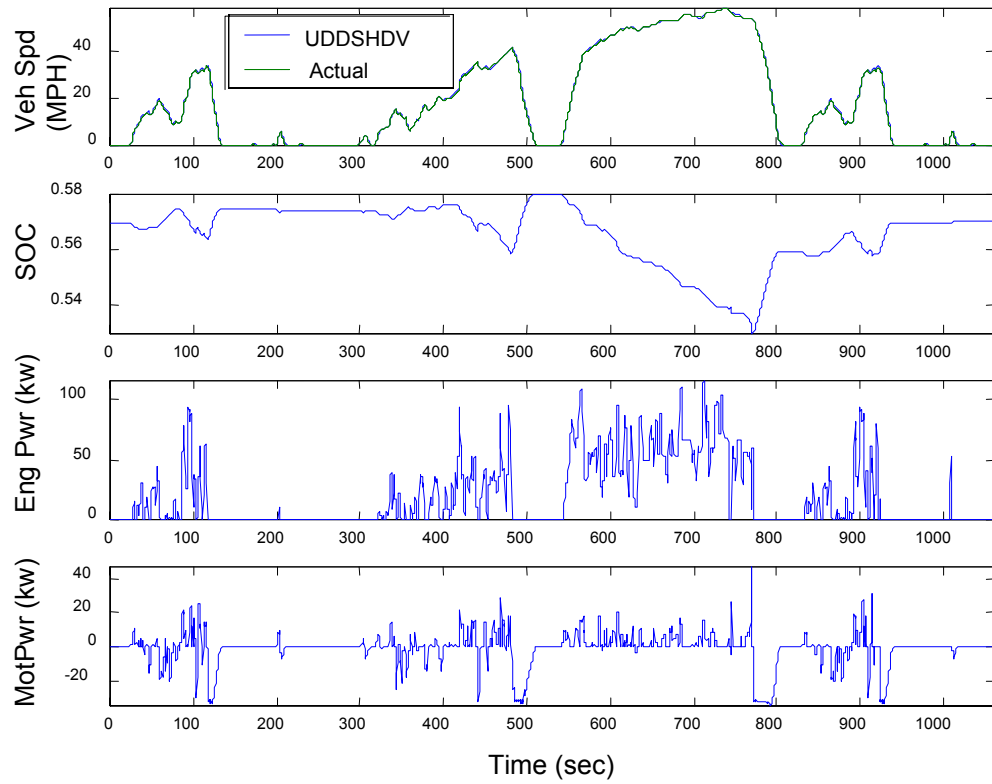


Power Management Strategy for a Parallel Hybrid Electric Truck

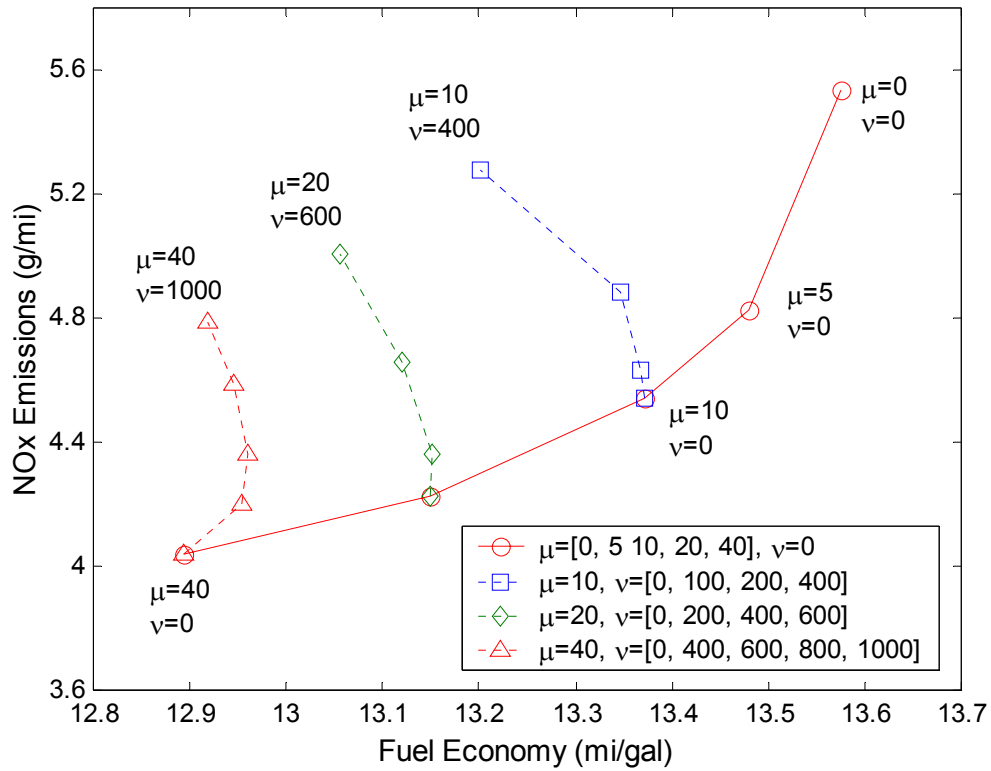
Chan-Chiao Lin, Huei Peng, J.W. Grizzle and Jun-Mo Kang: Figure 6



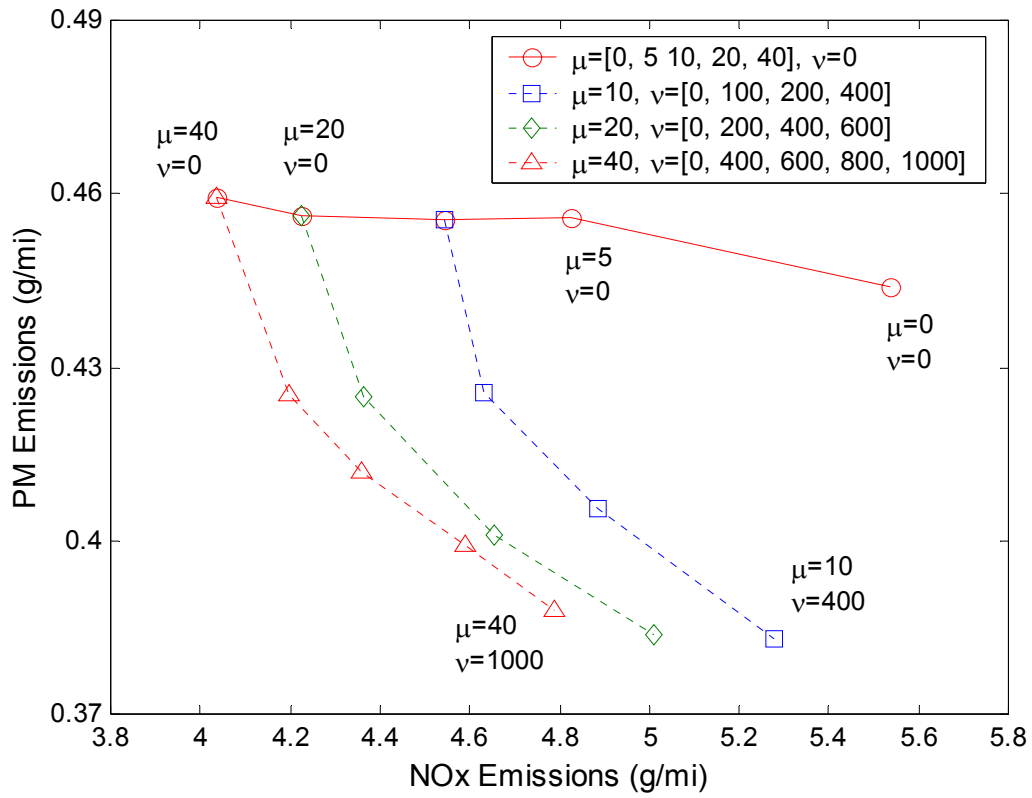
Chan-Chiao Lin, Huei Peng, J.W. Grizzle and Jun-Mo Kang: Figure 7



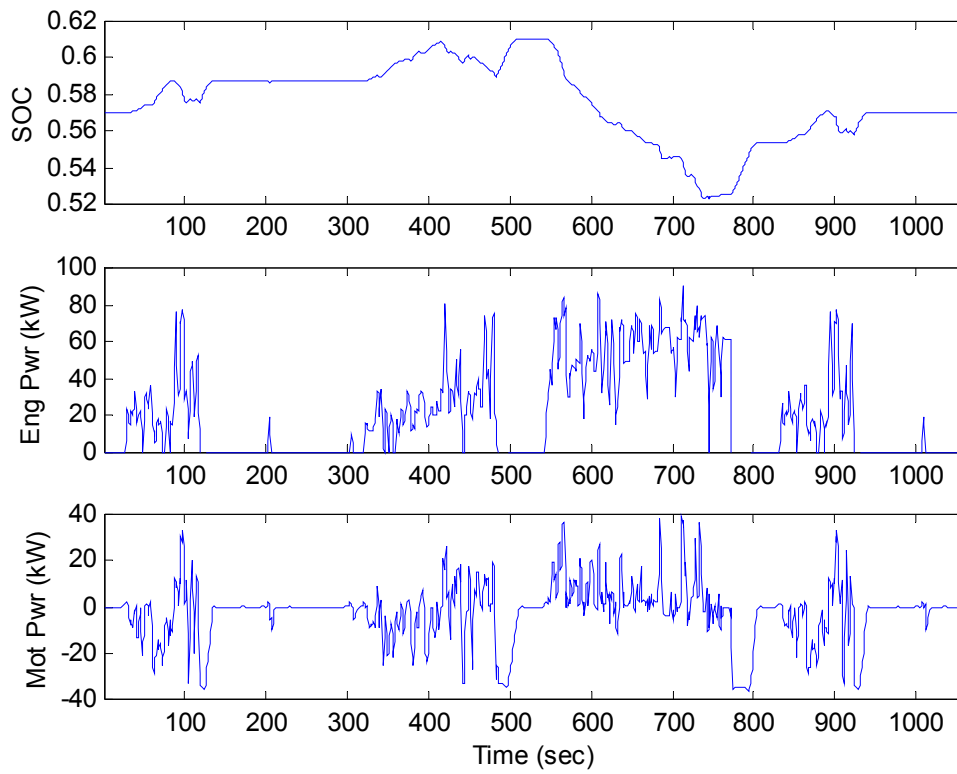
Chan-Chiao Lin, Huei Peng, J.W. Grizzle and Jun-Mo Kang: Figure 8



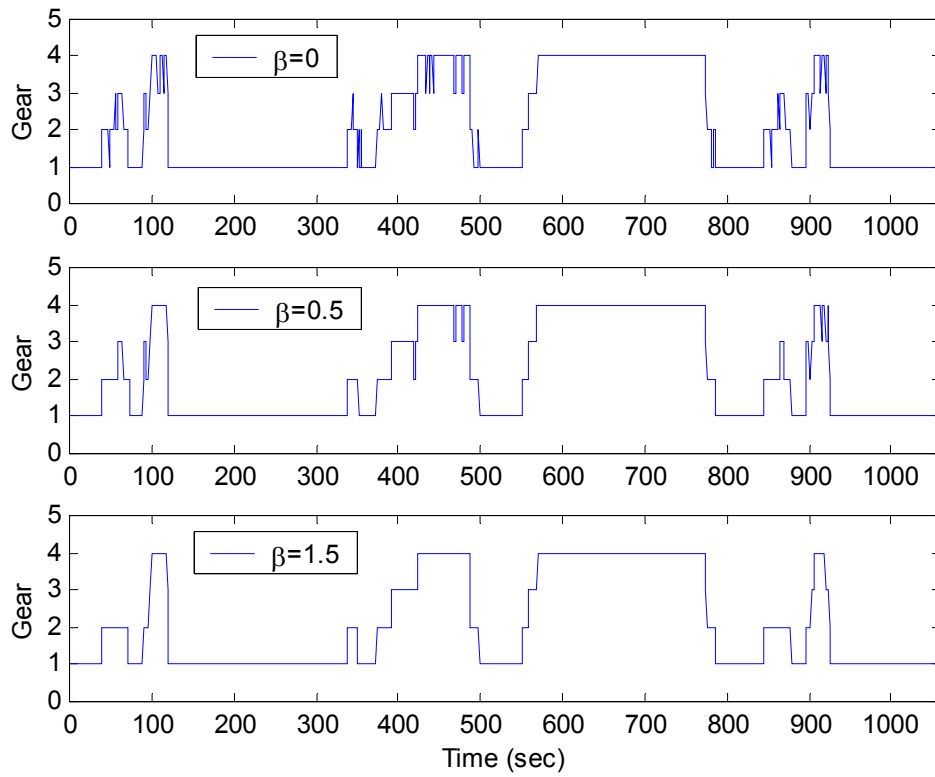
Chan-Chiao Lin, Hwei Peng, J.W. Grizzle and Jun-Mo Kang: Figure 9



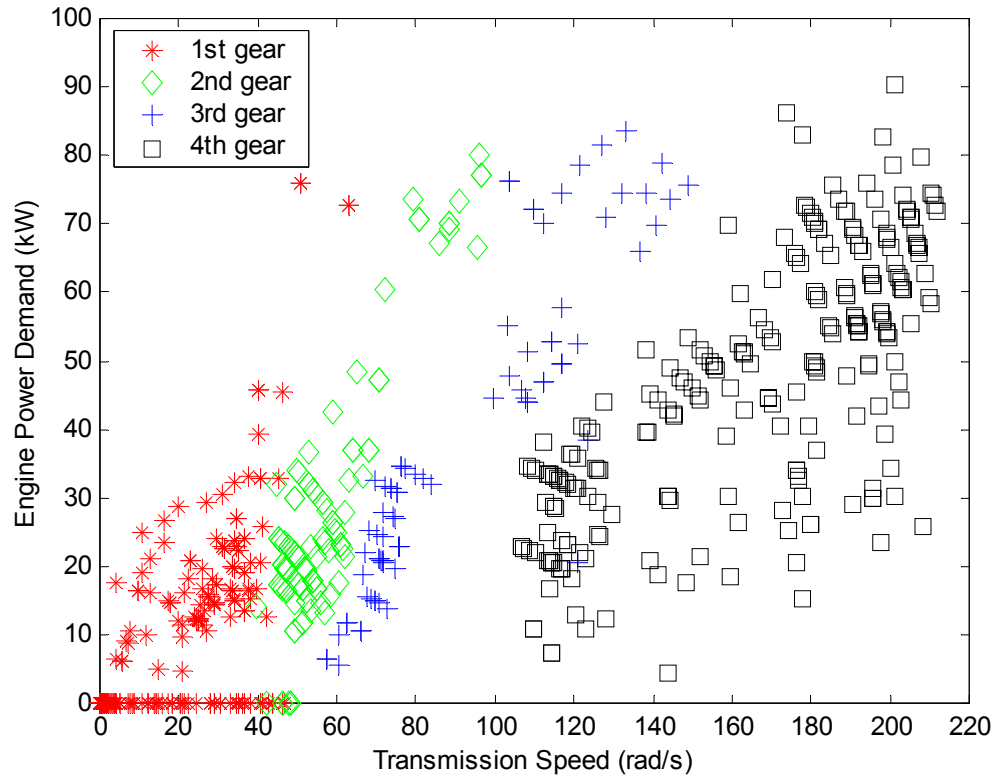
Chan-Chiao Lin, Huei Peng, J.W. Grizzle and Jun-Mo Kang: Figure 10



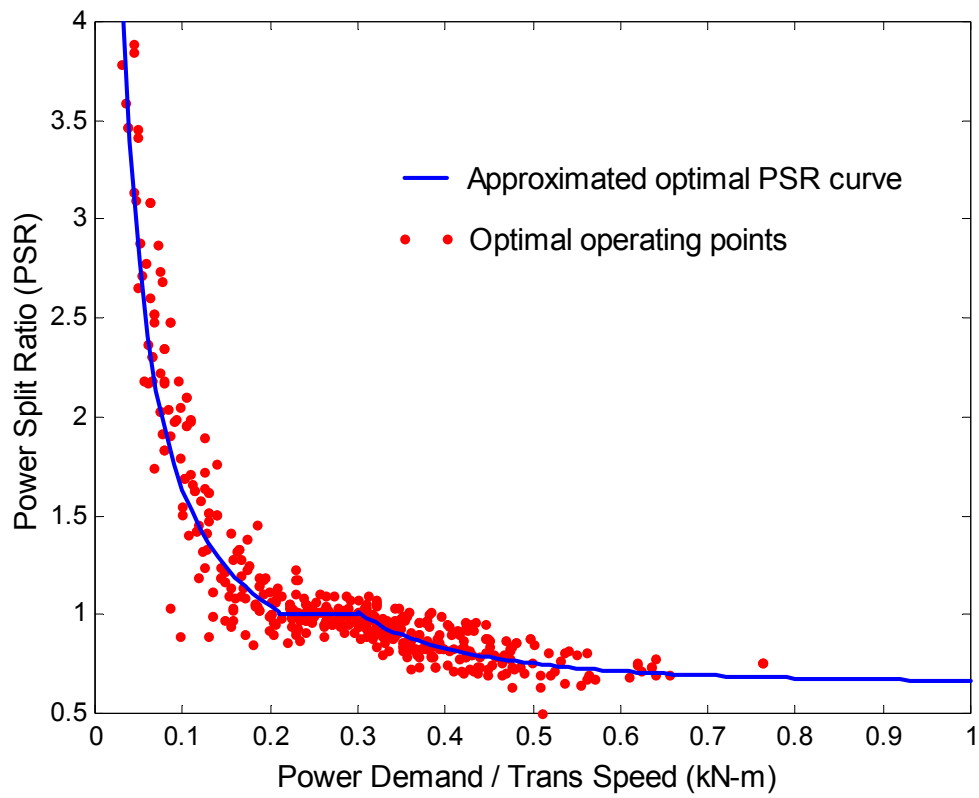
Chan-Chiao Lin, Hwei Peng, J.W. Grizzle and Jun-Mo Kang: Figure 11



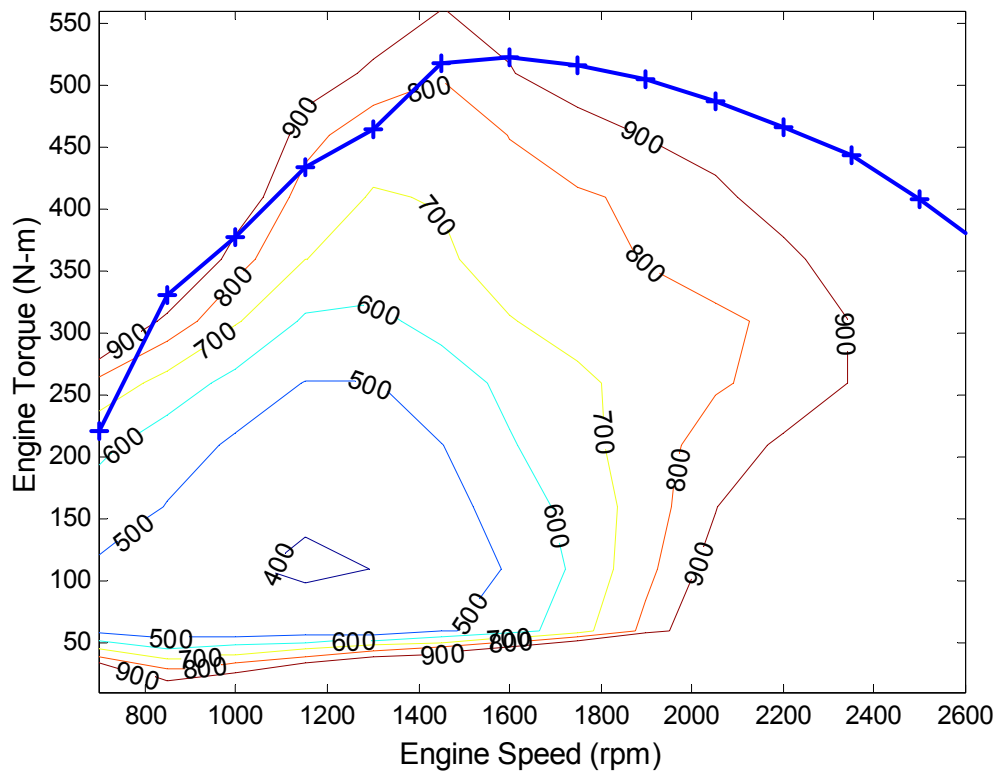
Chan-Chiao Lin, Hwei Peng, J.W. Grizzle and Jun-Mo Kang: Figure 12



Chan-Chiao Lin, Huei Peng, J.W. Grizzle and Jun-Mo Kang: Figure 13



Chan-Chiao Lin, Hwei Peng, J.W. Grizzle and Jun-Mo Kang: Figure 14



Chan-Chiao Lin, Huei Peng, J.W. Grizzle and Jun-Mo Kang: Figure 15

